nature biomedical engineering

Supplementary information

https://doi.org/10.1038/s41551-025-01597-0

Digital CRISPR-based diagnostics for quantification of *Candida auris* and resistance mutations

In the format provided by the authors and unedited

Supplemental Information to "Digital CRISPR-based diagnostics for quantification of *Candida auris* and resistance mutations".

Table of Contents

Supplemental Tables 2
SI Table 1. Molecular concentration per compartment 2
SI Table 2. Sequences of synthetic nucleic acids 2
SI Table 3. DNA extracted from culture samples for specificity testing 5
SI Table 4. Buffer compositions 6
SI Table 5. Amies medium composition 6
SI Table 6. Extracted Features 7
SI Table 7. Primer Analysis by Clades 8
SI Table 8. Molecular characteristics of clinical surveillance swabs 10
Supplemental Figures and Discussion 11
SI Fig 1. Schematic representation of the digital SHERLOCK methodology. 11
SI Fig 2. Primary and secondary screening of RPA primer pairs. 12
SI Fig 3. Optimization of buffer composition for dSHERLOCK 14
SI Fig 4. Distributions of maximum fluorescence intensity for compartments of chips loaded with 50fM *C. auris* sample. 15
SI 1. Detailed discussion of calibration curves for dSHERLOCK *C. auris* and FKS1 assay 15
SI 2. Quantification of fungal load in simulated clinical samples 16
SI Fig 5. Effects of clinical swab sample transport medium (Amies) and HEK293FT cell-extracted genomic DNA (hgDNA) on absolute quantification of synthetic *C. auris* target DNA with dSHERLOCK. 17
SI Fig 6. % Positive partitions for a range of reaction times before compartmentalization. 18
SI Fig 7. dSHERLOCK performance on blinded accuracy panel of simulated swab samples in Amies medium and comparison to common quantitative methods. 18
SI 3. Detailed discussion of comparison between quantifications by dSHERLOCK, ddPCR, and qPCR in terms of CFU. 18
SI Fig 8. Selection of optimal fluorescence threshold dSHERLOCK assays for *C auris* with clinical swabs. 19
SI Fig 9. Outlier detection on dSHERLOCK quantification of C. auris in clinical swabs. 20
SI Fig 10. Optimization of SHERLOCK FKS1 and ERG11 assay one pot reactions through engineered mutations. 21
SI Fig 11. dSHERLOCK FKS1 assay fluorescence intensity over time 22
SI Fig 12. Batch effects prohibit the use of thresholds for robust differentiation between alleles. 23
SI Fig 13. Feature extraction and labelling of negative compartments via GRANITE (Gaussian Robust Algorithm for Negative Identification via Thorough Estimation) 24
Bibliography 24

Supplemental Tables

SI Table 1. Molecular concentration per compartment

Molecule	Initial number of molecules in each microwell
Forward primer	2×10^{10}
Reverse primer	2×10^{10}
Lba Cas12a	2×10^{9}
gRNA	4×10^{11}
FQ (fluorophore-quencher reporter molecule)	5×10^{10}
MgOAc	6×10^{14}
DNA target	Variable (mostly 0 or 1)

SI Table 2. Sequences of synthetic nucleic acids

Description	Sequence
Candida auris target DNA	gcgctaatacgactcactatagggtccgtaggtgaacctgcggaaggatcattattgatattttgcatacacactgatttgg attttaaaactaacccaacgttaagttcaactaaaacaaaaacataaaactttcaacaacggatctcttggttctcgcatcg atgaagaacgcagcgaaatgcgatacgtagtatgacttgcagacgtgaatcatcgaatctttgaacgcacattgcgcctt ggggtattccccaaggcatgcctgtttgagcgtgatgtcttctcaccaatcttcgcggtggcgttgcattcacaaaattaca gcttgcacgaaaaaaatctacgctttttttttcgttttgttgtcgcctcaaatcaggtaggactacccgctgaacttaagcata tcaataagcggaggaaaaga
FKS1 mutant target DNA (S639F mutation)	gcgctaatacgactcactataggggtatctattgttgggttcttcattgctgtcgctaccttgcttttcttcgctatcatgccttt gggtggcttgttcacatcttacatgaacagaagatcaagaaagtacgtggcatcccaaattttcactgcaaatttccactct ttgaggggcttggacatgtggatgtcttaccttctttgggtcactgtgtttgctgctaagttggccgaatcttacttcttcttga ctttgtTcttgagagatcctattagaaacttgtccaccatgacgatgagatgcaacggtgaacaatggtttggtgatacctt gtgtaaacaccaggccaagattgtcttgggcttgatgcttcttgtcgatttgttcttgttcttcttggatacttacatgtggtac attatttgtaactgtgttttctccattggtcgttcgttctacttgggtatttctatcttgaccc
FKS1 wildtype target DNA	gcgctaatacgactcactataggggtatctattgttgggttcttcattgctgtcgctaccttgcttttcttcgctatcatgccttt gggtggcttgttcacatcttacatgaacagaagatcaagaaagtacgtggcatcccaaattttcactgcaaatttccactct ttgaggggcttggacatgtggatgtcttaccttctttgggtcactgtgtttgctgctaagttggccgaatcttacttcttcttga ctttgtCcttgagagatcctattagaaacttgtccaccatgacgatgagatgcaacggtgaacaatggtttggtgatacctt gtgtaaacaccaggccaagattgtcttgggcttgatgcttcttgtcgatttgttcttgttcttcttggatacttacatgtggtac attatttgtaactgtgttttctccattggtcgttcgttctacttgggtatttctatcttgaccc
ERG11 mutant target DNA (Y132F and K143R mutations)	gcgctaatacgactcactataggggccatatcaatttttcgagctgtgcagagagaaatacggcgatgtgtttgctttcgt gatgttaggaaaagttatgacggtttacttgggacctaagggacacgagtttgtattgaacgcaaagcttgcggatgtttct gccgaggctgcttattcccacttgaccactccagttttcgggaaaggtgtcatttTcgactgtcccaactcgaggttgatg gagcagaGgaaatttgctaagactgccttgacgaaagaggcttttcagaggtacgtgcctagaatccaagaggaagta ttggactacttcaaagcttgctcccaattcagaatgaacgaacgtaacaacggcgtggccaatgtgatgaagactcaac ctgagatgaccatcttaactgcttccaagtcgttgatgggtgatgacatgagagccagatttgatgcctccttcgccaaatt g
ERG11 wildtype target DNA	gcgctaatacgactcactataggggccatatcaatttttcgagctgtgcagagagaaatacggcgatgtgtttgctttcgt gatgttaggaaaagttatgacggtttacttgggacctaagggacacgagtttgtattgaacgcaaagcttgcggatgtttct gccgaggctgcttattcccacttgaccactccagttttcgggaaaggtgtcatttAcgactgtcccaactcgaggttgatg gagcagaAgaaatttgctaagactgccttgacgaaagaggcttttcagaggtacgtgcctagaatccaagaggaagta

	ttggactacttcaaagcttgctcccaattcagaatgaacgaacgtaacaacggcgtggccaatgtgatgaagactcaac ctgagatgaccatcttaactgcttccaagtcgttgatgggtgatgacatgagagccagatttgatgcctccttcgccaaatt g
Scrambled target DNA	aatttatctgcaccaccggcaaactgccggtgccgtggccgacgctggtgaccaccctgacctatggcgttcagtgtttt agtcgctatccggatcacatgaaacgtcacgatttctttaaatctgcaatgccggaaggctatgtgcaggaacgtacgatt agctttaaagatgatggcaaatataaaacgcgcgccgttgtgaaatttgaaggcgataccctggtgaaccgcattgaact gaaaggcacggattttaaagaagatggcaatatcctgggccataaactggaatacaactttaatagccataatgtttatatt acggcggataaacagaaaaatggcatcaaagcgaattttaccgttcgccataacgttgaagatggcagtgtgcagctg gcagatcattatcagcagaataccccgattggtgatggtccggtgctgctgccggataatcattatctgagcacgcagac cgt
DNA used to make *C. auris* matched gRNA with T7 promoter	cacaaaattacagcttgcacatctacacttagtagaaattaccctatagtgagtcgtattagcgc
DNA used to make *C. auris* mismatched gRNA with T7 promoter	5bp mismatch: cacaaaattacagct**G**gcacatctacacttagtagaaattaccctatagtgagtcgtattagcgc 9bp mismatch: cacaaaattac**G**gcttgcacatctacacttagtagaaattaccctatagtgagtcgtattagcgc 15bp mismatch: cacaa**G**attacagcttgcacatctacacttagtagaaattaccctatagtgagtcgtattagcgc
DNA used to make FKS1 mutation (S639F) matched gRNA with T7 promoter	ctaataggatctctcaagAaatctacacttagtagaaattaccctatagtgagtcgtattagcgc
DNA used to make FKS1 mutation (S639F) mismatched gRNA with T7 promoter	ctaataggatctctcaGgAaatctacacttagtagaaattaccctatagtgagtcgtattagcgc
DNA used to make ERG11 (Y132F) mutation matched gRNA with T7 promoter	aacctcgagttgggacagtcatctacacttagtagaaattaccctatagtgagtcgtattagcgc
DNA used to make ERG11 mutation mismatched gRNA with T7 promoter	aacctcgagttgggacGgtcatctacacttagtagaaattaccctatagtgagtcgtattagcgc
T7 primer	gcgctaatacgactcactatagg
Candida auris forward primer	Selected after secondary screen (final): gaatctttgaacgcacattgcgccttggggtatt Primary screen: agacgtgaatcatcgaatctttgaacgcacatt
Candida auris reverse primer	Selected after secondary screen (final): attgatatgcttaagttcagcgggtagtccta Primary screen: cctccgcttattgatatgcttaagttcagcgggta
FKS1 forward primer	ttgctgctaagttggccgaatcttacttct
FKS1 reverse primer	atcgacaagaagcatcaagcccaagacaat

ERG11 forward primer	gccgaggctgcttattcccacttgaccact
ERG11 reverse primer	tccaatacttcctcttggattctaggcacgta
Fluorophore-quenched ssDNA fluorescent reporter	56-fam/ttatt/3iabkfq

SI Table 3. DNA extracted from culture samples for specificity testing

Species	Concentration (ng/µL)	NCBI Accession
Candida auris, Clade 1 (S. Asian)	60	MW040020
Candida auris, Clade 1 (S. Asian)	130	MW040021
Candida auris, Clade 2 (E. Asian)	155	MW040022
Candida auris, Clade 2 (E. Asian)	119	MW040023
Candida auris, Clade 3 (S. Af)	52	MW040024
Candida auris, Clade 4 (S. Am)	134	MW040025
Candida auris, Clade 4 (S. Am)	107	MW040026
Candida duobushaemulonii	20	MW040032
Candida famata	13	MW040033
Candida orthopsilosis	38	MW040034
Candida tropicalis	31	MW040036
Candida blankii	38	MW040037
Candida ciferrii	25	MW040038
Candida colliculosa	30	MW040039
Candida dubliniensis	40	MW040040
Candida fabianii	35	MW040041
Cryptococcus diffluens	19.5	MW040042
Pichia norvegensis	58	MW040044
Cryptococcus albidus	31.9	MW040045
Debaromyces hansenii	38	MW040046
Cryptococcus neoformans	11.5	MW040047
Candida krusei	25	MW040027
Candida parapsilosis	27	MW040028
Candida glabrata	49	MW040029
Candida albicans	55	MW040030
Candida lusitaniae	25	MW040031
Candida haemulonii	28	MW040035
Saccharomyces cerevisiae	44	MW147741
Malasezzia pachydermata	30	MW147742
Malasezzia furfur	10	MW147743

SI Table 4. Buffer compositions

Buffer	Component	Molarity [M]	Weight/volume	Notes
1	HEPES (pH 6.8)	0.02		
	PEG-8k		0.05	
	NaCl	0.06		
2	Same as 1 (new preparation)			
3	Proprietary (TwistDx TwistAmp Basic Kit RPA rehydration buffer)			Contains Tris, high molecular weight PEG and NaCl[1]
4	Tris (tris(hydroxymethyl)aminomethane (pH 8.19)	0.02		
	NaCl	0.06		
	PEG-35k		0.05	
5	Tris (tris(hydroxymethyl)aminomethane (pH 8.19)	0.02		
	NaCl	0.06		
	PEG-35k		0.05	
	Polysorbate 20		0.005	

SI Table 5. Amies medium composition

Component	Concentration [g/l]
Sodium Chloride	3
Potassium Chloride	0.2
Disodium Phosphate	1.15
Calcium Chloride	0.1
Sodium Thioglycolate	1.0
Magnesium Chloride	0.1
Dipotassium Phosphate	0.2
Agar	4

SI Table 6. Extracted Features

Name	Explanation
feat_fq_delta_final_corr	Intensity at last timepoint
feat_fq_delta_max_corr	Maximum intensity
feat_fq_delta_avg_corr	Average intensity
feat_fq_delta_area_final_corr	Area under the curve
feat_fq_delta_velocity_final_corr	Velocity at last timepoint
feat_fq_delta_velocity_max_corr	Maximum velocity
feat_fq_delta_velocity_min_corr	Minimum velocity
feat_fq_delta_velocity_avg_corr	Average velocity
feat_fq_delta_tp_max	Timepoint of maximum intensity
feat_fq_delta_tp_min	Timepoint of minimum intensity
feat_fq_delta_tp_avg	Timepoint of surpassing average intensity
feat_fq_delta_velocity_tp_max	Timepoint of maximum velocity
feat_fq_delta_velocity_tp_min	Timepoint of minimum velocity
feat_fq_delta_velocity_tp_avg	Timepoint of first surpassing average velocity
feat_tp_start_active	Timepoint of first surpassing 50% of maximum velocity

SI Table 7. Primer Analysis by Clades

All "Complete" strains in NCBI	Clade	Strains with >=1 locus with exact match to current study primers and gRNA	Strains with >=1 locus with exact match to Leach *et al.* V2424/5/6 primers	Strains not matched to current study primers and gRNA	Strains not matched to Leach *et al*. V2424/5/6 primers
470140	1	470140	470140	CA2LBN	CA2LBN
A1	3	A1	A1	CA4LBN	CA4LBN
B11103	1	B11103	B11103	CA6LBN	CA6LBN
B11205	1	B11205	B11205	CA9LBN	CA9LBN
B11220	2	B11220	B11220	CA14LBN	CA14LBN
B11221	3	B11221	B11221	CA19LBN	CA19LBN
B11244	4	B11244	B11244	CA21LBN	CA21LBN
B11245	4	B11245	B11245	CA24LBN	CA24LBN
B11809	2	B11809	B11809	CA25LBN	CA25LBN
B12037	3	B12037	B12037	CA29LBN	CA29LBN
B12043	2	B12043	B12043		
B12342	4	B12342	B12342		
B12631	3	B12631	B12631		
B13463	2	B13463	B13463		
B13916	1	B13916	B13916		
B17721	3	B17721	B17721		
B8441	1	B8441	B8441		
CA10LBN	1	CA10LBN	CA10LBN		
CA11LBN	1	CA11LBN	CA11LBN		
CA12LBN	1	CA12LBN	CA12LBN		
CA13LBN	1	CA13LBN	CA13LBN		
CA14LBN	1	CA15LBN	CA15LBN		
CA15LBN	1	CA16LBN	CA16LBN		
CA16LBN	1	CA17LBN	CA17LBN		
CA17LBN	1	CA18LBN	CA18LBN		
CA18LBN	1	CA1LBN	CA1LBN		
CA19LBN	1	CA20LBN	CA20LBN		
CA1LBN	1	CA22LBN	CA22LBN		
CA20LBN	1	CA23LBN	CA23LBN		
CA21LBN	1	CA26LBN	CA26LBN		
CA22LBN	1	CA27LBN	CA27LBN		
CA23LBN	1	CA28LBN	CA28LBN		
CA24LBN	1	CA5LBN	CA5LBN		
CA25LBN	1	CA7LBN	CA7LBN		
CA26LBN	1	CA8LBN	CA8LBN		
CA27LBN	1	CAAM1	CAAM1		
CA28LBN	1	F1580	F1580		
CA29LBN	1	F3485	F3485		
CA2LBN	1	IFRC2087	IFRC2087		

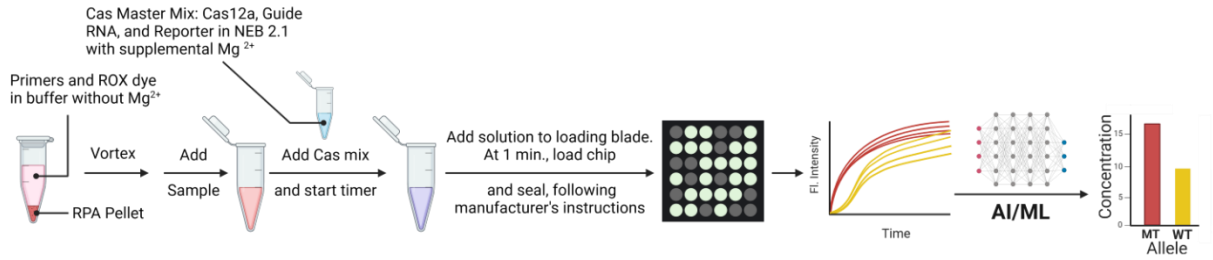
CA4LBN	1	LMDM 1219	LMDM 1219		
CA5LBN	1				
CA6LBN	1				
CA7LBN	1				
CA8LBN	1				
CA9LBN	1				
CA-AM1	1				
F1580	6				
F3485	6				
IFRC2087	5				
LMDM 1219	4				

Candida auris has 50 completely assembled genomes in NCBI, representing 49 strains and all clades. The ITS region is between the small and large subunit rRNA genes, and these are regions often duplicated across several of its seven chromosomes. Most strains of *C. auris* have 5-20 copies of this region typically spread across 3-4 chromosomes. Alignments (see included full alignment FASTA file) of these areas show that our assay performs identically to the standard qPCR assay by Leach *et al*. Both assays had perfect matches to 49 strains spanning all clades (see SI Table 7). However, both the Leach *et al*. qPCR assay and our assay, which it follows, had significant binding differences to ten clade 1 strain sequences submitted by the Molecular Mycology Laboratory in Bangalore, India (https://www.ncbi.nlm.nih.gov/pmc/articles/PMC9045239/). The exact nature of the differences in these specific genomes is beyond the scope of this paper, but our approach is easily adaptable including designing either clade-specific targets, as suggested here, or updated universal targets if the sequences of these ten clade 1 strains are confirmed.

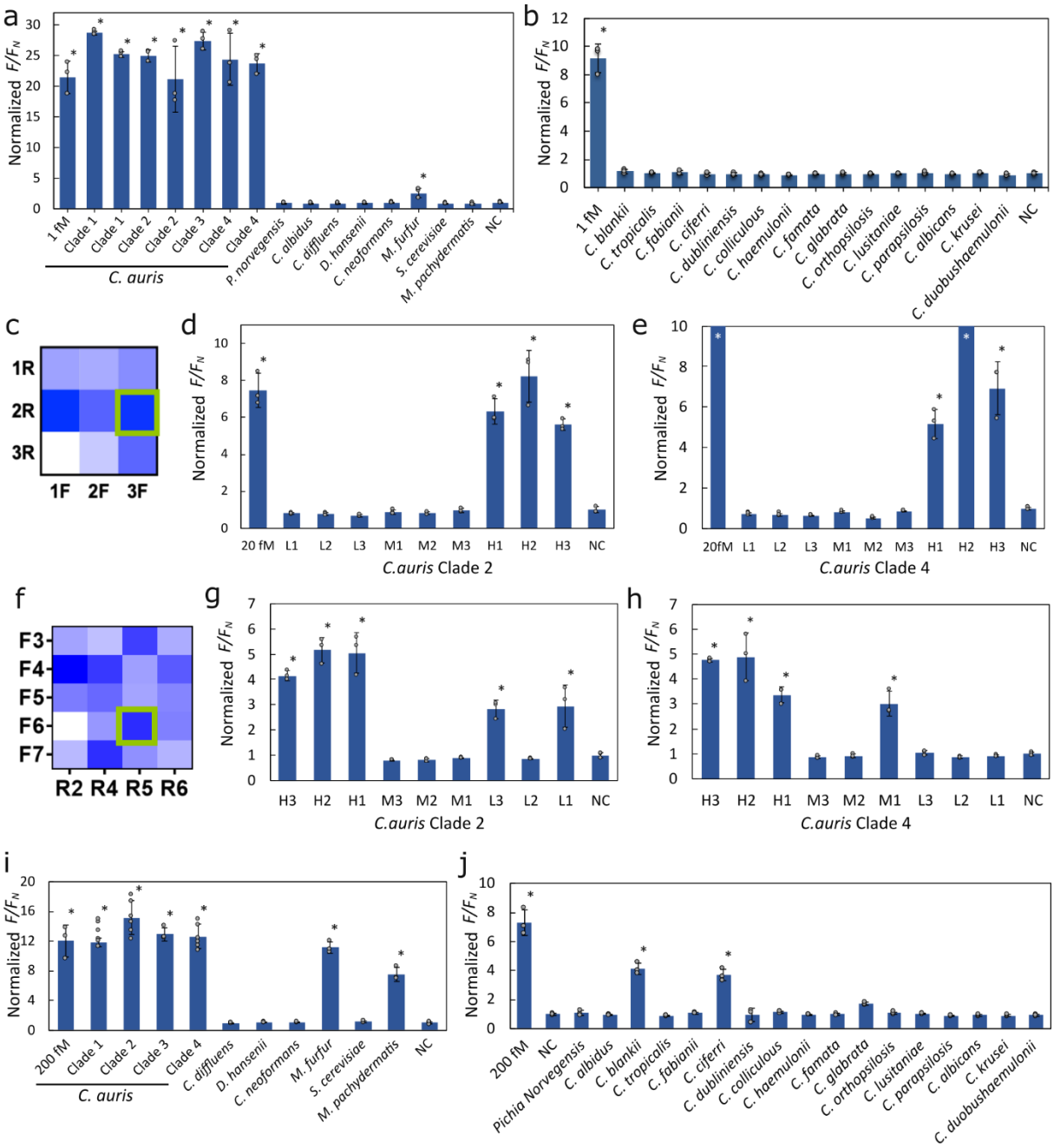
SI Table 8. Molecular characteristics of clinical surveillance swabs

Blinded ID	Wadsworth Ct	Chromagar Candida Plus (Predictive ID)	MALDI results
Swab 1	Undet	Not cultured	NA
Swab 2	26.3	Blue halo/pink - abundant (C. auris), Metal Blue (C. tropicalis)	C. auris 2.48/2.40
Swab 3	Undet	Not cultured	NA
Swab 4	Undet	Not cultured	NA
Swab 5	23.1	Blue halo/pink - abundant (C. auris)	C. auris 2.59/2.52
Swab 6	Undet	Not cultured	NA
Swab 7	26.5	Blue halo/pink - abundant (C. auris), Metal Blue (C. tropicalis), mauve (C. glabrata)	C. auris 2.03/2.02
Swab 8	Undet	Not cultured	NA
Swab 9	26.5	Blue halo/pink - abundant (C. auris), mauve (C. glabrata)	C. auris 2.32/2.25
Swab 10	Undet	Not cultured	NA
Swab 11	19.8	Blue halo/pink - abundant (C. auris)	C. auris 2.34/2.33
Swab 12	28.9	Blue halo/pink - 4 colonies (C. auris), blue-green (C. albicans)	C. auris 2.42/2.35
Swab 13	Undet	Not cultured	NA
Swab 14	Undet	Not cultured	NA
Swab 15	Undet	Not cultured	NA
Swab 16	20.5	Blue halo/pink - abundant (C. auris)	C. auris 2.48
Swab 17	Undet	Not cultured	NA
Swab 18	20.7	Blue halo/pink - abundant (C. auris)	C. auris 2.46/2.45
Swab 19	23	Blue halo/pink - abundant (C. auris), blue-green (C. albicans), Metal Blue (C. tropicalis)	C. auris 2.58
Swab 20	23.2	Blue halo/pink - abundant (C. auris)	C. auris 2.32
Swab 21	Undet	Not cultured	NA
Swab 22	31.6	Blue halo/pink - abundant (C. auris), Blue halo/pink irregular (C. parapsilosis), Metal Blue (C. tropicalis), mauve (C. glabrata)	C. auris 2.61
Swab 23	32.4	Blue halo/pink - abundant (C. auris), blue-green (C. albicans), mauve (C. glabrata)	C. auris 2.47
Swab 24	32.5	Blue halo/pink - 4 colonies (C. auris)	C. auris 2.30
Swab 25	Undet	Not cultured	NA
Swab 26	29	Blue halo/pink - abundant (C. auris), small blue (bacteria)	C. auris 2.51/2.45
Swab 27	Undet	Not cultured	NA
Swab 28	29.3	Blue halo/pink - abundant (C. auris), pink halo/metal blue (C. tropicalis), brown (bacteria)	C. auris 2.43
Swab 29	Undet	Not cultured	NA
Swab 30	Undet	Not cultured	NA

Supplemental Figures and Discussion

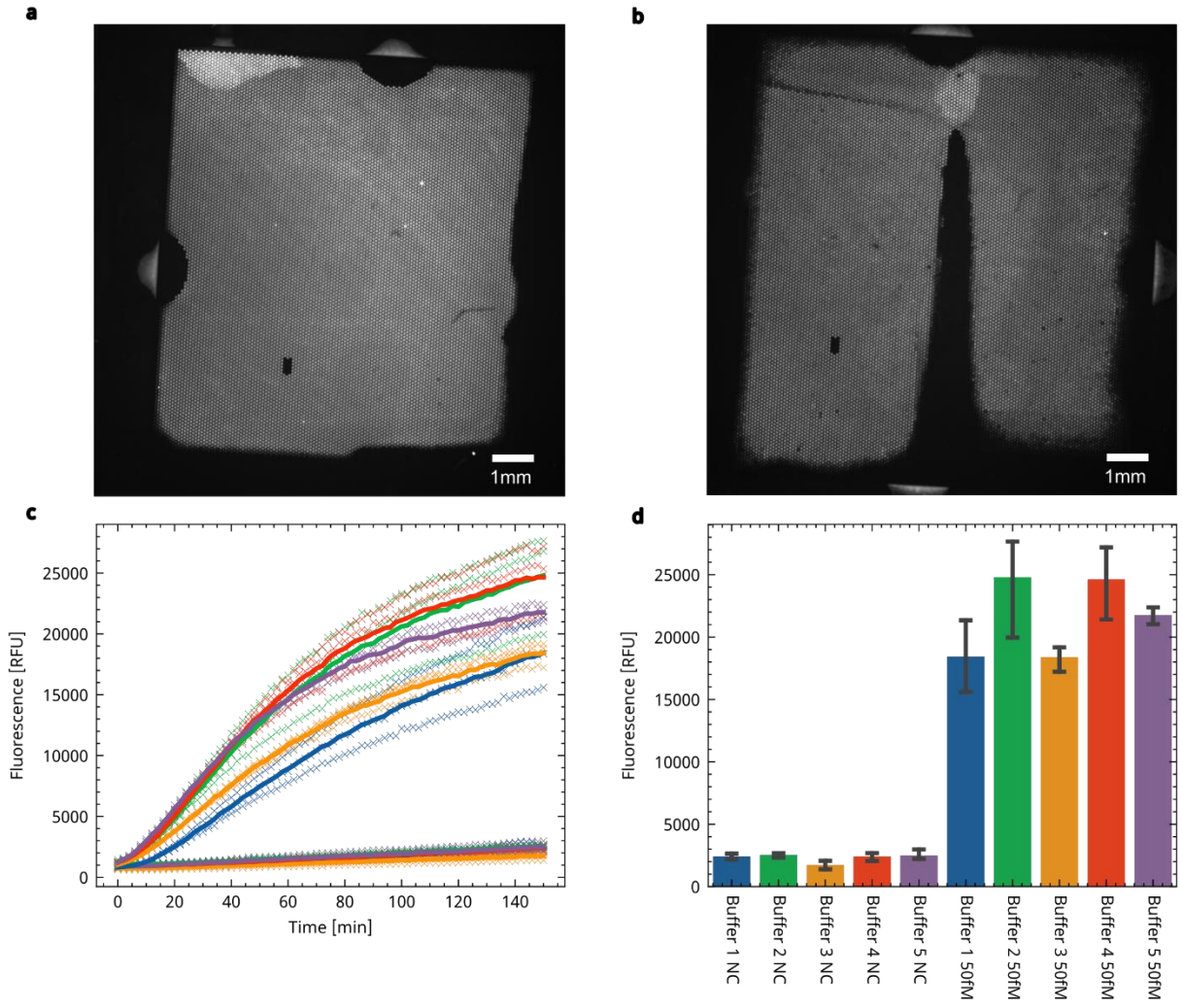


SI Fig 1. Schematic representation of the digital SHERLOCK methodology. Created in BioRender. (2025) https://BioRender.com/u50n390

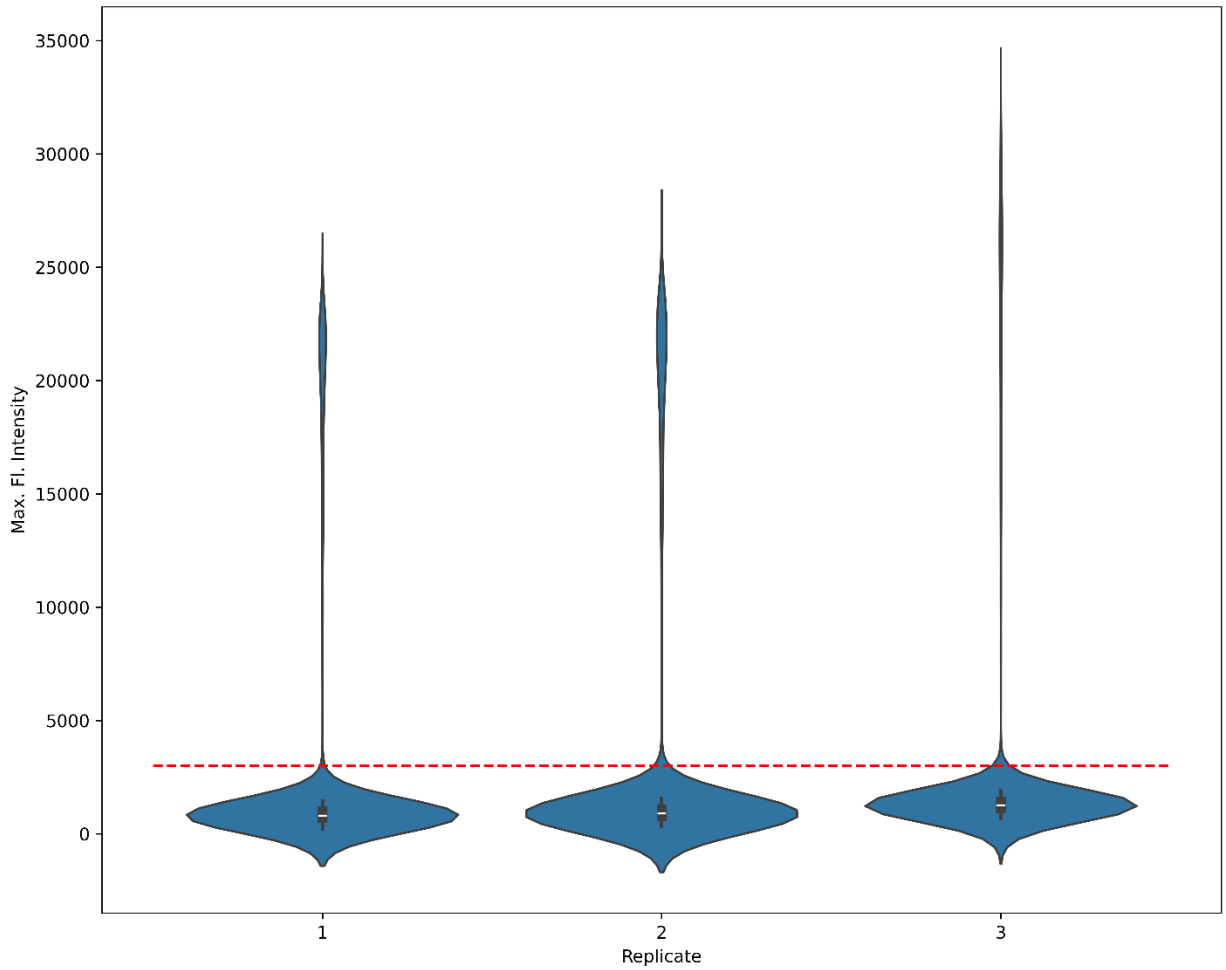


SI Fig 2. Primary and secondary screening of RPA primer pairs. a-b, Initial screen of the assay using RPA primers from a primary screen to detect **four major** Clades of *C. auris* and not detect closely related yeast from a specificity panel. These results were performed with Twist Dx Liquid RPA kits according to kit protocols. However, for assay stability it is preferred to use the lyophilized solid RPA kits as described in the main manuscript methods. **c**, Primary solid RPA primer screen including the same primers (F3-R2) used in a-b demonstrating that they remain top primer candidates in the solid RPA assay, **d-e,** Sensitivity for detecting *C. auris* Clade 2 and 4 using solid RPA and the primary screen primer pair (2R-3F). Only high concentrations of *C. auris* result in signal significantly higher than the negative control (NC), motivating a secondary primer screen as per Twist Dx primer design guidelines to improve sensitivity. In panel e, white stars on 20 fM and H2 samples indicate measurements that exceeded the fluorescence range of the instrument. **f-j,** results from a secondary RPA primer screen with **g-h**, sensitivity for detecting *C. auris* Clade 2 and 4 demonstrating the detection of some moderate or low concentrations. High concentration *C. auris* is used as a

positive control in these experiments. Sensitivity was further improved before results presented in the manuscript through optimizing mixing of samples and increasing reaction volume before collecting results shown in Figure 1. **i-j,** Detection of 4 Clades of *C. auris* and specificity panel for primer pair selected from the secondary screen (F6-R5). Two isolates were available for testing our ability to detect Clades 1, 2, 4 of *C. auris*- in these cases and the NC, the results are the mean of two samples, each measured as technical triplicates (n=6). Some false positives were detected in the specificity panel, however the primers from the secondary screen provided sensitivity advantages and it was anticipated that the digital assay system would help reduce the impact of any false positives through the ability to isolate any cross-contaminants in an individual well as well as differentiate non-specific reactions based on reaction kinetics. Primer sequences are in SI Table 1 and information on specificity panel is in SI Table 1.5. Unless otherwise noted, for all measurements in **Fig SI2 a-j:** measurements were performed as technical triplicates (n=3) with error bars representing one standard deviation above and below the mean; fluorescence signal (F) is normalized to the mean of the negative control (F_N); using a threshold of $F/F_N > 2$, positive signals have been marked with an *; NC- negative control; samples labelled in fM are positive controls of *C. auris* synthetic DNA.



SI Fig 3. Optimization of buffer composition for dSHERLOCK. a-b, buffer optimized for tube-scale assays causes suboptimal loading of microarray such as **(a)** interconnected microwells **(b)** poor wetting of chip surface. **c-d,** buffer optimized for dSHERLOCK leads to **(c)** improved bulk kinetics (blue: buffer 1, green: buffer 2, orange: buffer 3, red: buffer 4, purple: buffer 5) and **(d)** improved end-point fluorescence. Error-bars indicate standard deviation, n=3 technical replicates. Bar chart depicts mean +/- SD corresponding to the traces in subpanel c at the 150-min timepoint. Use of surfactant Polysorbate 20 does not significantly inhibit SHERLOCK reaction. Buffer compositions can be found in SI Table 2.



SI Fig 4. Distributions of maximum fluorescence intensity for compartments of chips loaded with 50fM *C. auris* sample. Initial fluorescence intensity was subtracted from the maximum fluorescence intensity reached in each compartment. By careful inspection, the maximum value observed in negative compartments did not exceed 3000 RFU (red dashed line). Based on this observation, a threshold of 3000 RFU was chosen to separate positive from negative compartments. n = 3 independent experiments.

SI 1. Detailed discussion of calibration curves for dSHERLOCK *C. auris* and FKS1 assays

A threshold of 3000 RFU was chosen for all chips. Three biological replicates were obtained at each concentration to estimate reproducibility. Background noise was estimated by recording chips with zero target DNA molecules in triplicate, taking the average percentage of compartments crossing over 3000 RFU and adding three times the standard deviation. A four-parameter logistic curve was fit to the data. The concentration at which the curve fell below the background noise was taken as the limit of detection (LOD)

C. auris:

The dSHERLOCK *C. auris* assay showed a dynamic range spanning four logs of target DNA concentrations, a linear range between approximately 1 fM and 100 fM, corresponding to about 3000 and 300,000 copies per 5 µL sample, and a LOD of about 100 aM or 300 copies in the sample. In chips used to

estimate background noise, between 0 and 3 compartments crossed the fluorescence intensity threshold and were therefore evaluated as positive, while in the lowest measured concentration, 500aM, the number of partitions turning 'on' were between 3 and 7. The curve fit resulted in an R^2 value of 0.98.

FKS1:

The dSHERLOCK *FKS1* assay had a dynamic range spanning four decades of target DNA concentrations for both the mutant and wildtype alleles. The linear range with respect to both target alleles was approximately between 100 aM and 10 fM and thereby ten-fold more sensitive than the dSHERLOCK *C. auris* assay. This linear range corresponded to between 60 and 6,000 copies per µL. Second, we evaluated the LOD of the assay. The definition of the LOD, as applied in the dSHERLOCK *C. auris* assay, was not applicable for the mutant allele of the dSHERLOCK *FKS1* assay. This was due to the background signal, defined as the mean of positive partitions between all negative control chips without DNA added to three times their standard deviation, being zero because no false positive partitions were detected in any of the three replicate chips. Therefore, the LOD was below the lowest measured concentration of 25 aM, or 75 copies in the sample. For the dSHERLOCK FKS1 assay used to detect the wildtype sequence, the earlier definition of the LOD was again applicable and led to the LOD of approximately 25 aM. The microarrays loaded without DNA were observed to have 1, 1, and 5 false positive partitions. The curve fit resulted in R^2 values of 0.72 and 0.99 for the mutant and the wildtype allele, respectively.

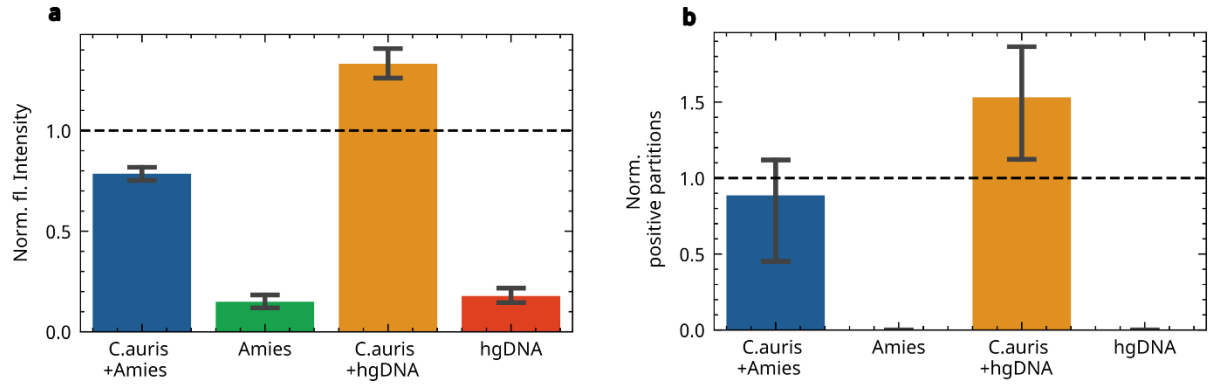
SI 2. Quantification of fungal load in simulated clinical samples

We assessed the ability of real-time dSHERLOCK to quantify *C. auris* from Amies medium and without interference from non-specific DNA or purification steps that would delay the identification of the pathogen and therefore appropriate response in terms of treatment and outbreak prevention measures. To test this capability, we selected 50 fM target DNA, a concentration in the middle of the linear range of the dSHERLOCK *C. auris* assay, and evaluated the impact of Amies media and non-specific DNA on the final fluorescence intensity in tube-scale reactions and the total number of positive partitions in dSHERLOCK (SI Fig. 2). A swab sample is expected to contain thousands of human skin cells per µL. In order to test robustness to a relatively high concentration of human skin cells, 100 ng/µL of genomic DNA (gDNA) extracted from human embryonic kidney 293FT (HEK293FT) cells was used in the sample (Invitrogen™ Thermo Fisher Scientific, MA, USA, Catalog #R70007). The cell lines was not independently authenticated. Cultures were tested for mycoplasma contamination using a commercial kit (Lonza MycoAlert, Catalog #T07-318) and were confirmed negative. This concentration corresponds to approximately 15 000 cell genomic equivalents per µL or 15 000 000 cells per swab. To note, gDNA was extracted from HEK293FT cells using Invitrogen™ PureLink™ Genomic DNA Mini Kit (Thermo Fisher Scientific, MA, USA). The concentration and purity of the extracted gDNA were measured using the absorbance-based nanodrop method. Amies medium was obtained from the BD ESwab Collection & Transport System. All samples were prepared in triplicate with separate reaction master mixes and run simultaneously for 2.5 h in both a 384-well plate and the dSHERLOCK platform. Results were normalized to measurements of *C. auris* in nuclease-free water.

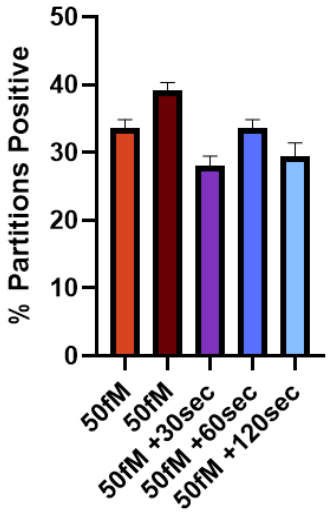
In the tube-scale reactions (384-well plate), a decrease in final fluorescence intensity of approximately 20% was observed in the positive sample containing Amies media with respect to the positive sample in

nuclease-free water. In contrast, HEK293FT gDNA resulted in an increase of approximately 30% final fluorescence intensity relative to the positive sample in nuclease-free water (SI Fig. 2a). While this result could indicate non-specific amplification, the reactions containing human genomic DNA without synthetic *C. auris* DNA did not show any signals visibly distinct from the reactions in the absence of DNA in Amies media. Thus, the observed effect is unlikely to occur from non-specific activation of the SHERLOCK reaction by HEK293FT gDNA. We hypothesize that the increase final fluorescence intensity in the presence of non-specific gDNA is the result of the excess DNA acting as a crowding agent to increase the efficiency of isothermal nucleic acid amplification, as has been observed by others[2].

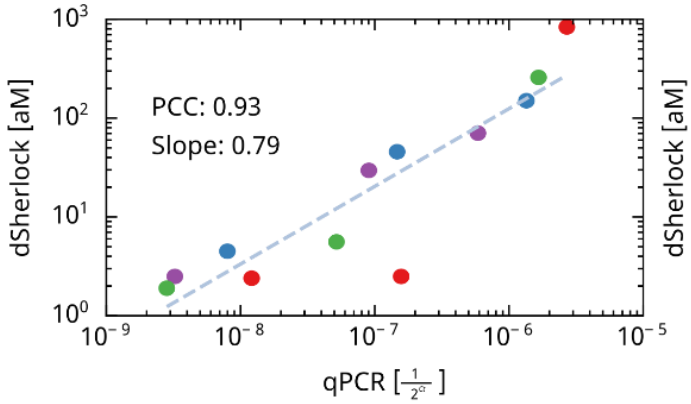
We next sought to evaluate the effect of media and non-specific DNA in a more quantitative manner using our dSHERLOCK pipeline (SI Fig. 4b). By distinguishing between presence/absence of a target molecule and reaction kinetics, we hypothesized that dSHERLOCK could distinguish between non-specific background and low efficiency cleavage of the reporter molecule. By contrast, these two effects are indistinguishable in tube-scale reactions. We did not detect a statistically different number of target molecules when the target DNA was in Amies media versus nuclease free water, indicating that Amies media would not inhibit quantification by dSHERLOCK. Similar to the tube-scale result, we observed an increase number of total partitions detected when the target DNA was in the presence of non-specific HEK293FT gDNA. In contrast, the reaction without target DNA, but including the non-specific gDNA, demonstrated fewer than three non-specific amplification events per array. Thus, we concluded that the increase in the number of positive partitions when including human genomic DNA in the sample was a result of more efficient recognition of individual target molecules, potentially achieved through a molecular crowding effect[2], rather than more efficient cleavage of the reporter molecules.



SI Fig 5. Effects of clinical swab sample transport medium (Amies) and HEK293FT cell-extracted genomic DNA (hgDNA) on absolute quantification of synthetic *C. auris* target DNA with dSHERLOCK. a, End-point fluorescence intensity of tube-scale SHERLOCK reactions after 2.5 h for samples of 50fM synthetic *C. auris* DNA in Amies medium (C.auris+Amies), pure Amies medium (Amies), 50 fM synthetic *C. auris* DNA with 100 ng/µL spiked genomic DNA (gDNA) extracted from HEK293FT cells in nuclease-free water (C.auris+hgDNA), and HEK293FT gDNA at a concentration of 100 ng/µL in nuclease-free water (hgDNA). Reactions were prepared in technical triplicate alongside batch control reactions with 50 fM synthetic *C. auris* DNA in nuclease-free water and fluorescence intensity was normalized to controls. **b,** dSHERLOCK positive partitions for samples from (a) as evaluated by a threshold of 3000 RFU after 2.5 h, normalized to positive partitions of batch controls. n = 3 independent experiments per condition.



SI Fig 6. % Positive partitions for a range of reaction times before compartmentalization. Measured values lack a statistical trend dependent on reaction time before compartmentalization. n=1 per condition, error bars indicate Poisson error. Statistical significance was tested using weighted linear regression, taking the inverse of the squared Poisson errors as weights for each measurement. *F*-statistic was found to be 1.4 with *p*-value = 0.32.



SI Fig 7. dSHERLOCK performance on blinded accuracy panel of simulated swab samples in Amies medium and comparison to common quantitative methods. dSHERLOCK results agree well with the clinical standard for quantitative nucleic acid detection quantitative PCR (qPCR). Curves were fit as linear functions minimizing the sum of squared errors. PCC (Pearson's correlation coefficient) was used to indicate goodness of fit. The sample preparation of simulated swab samples in the accuracy panel can be found in the methods section. n= 15 samples.

SI 3. Detailed discussion of comparison between quantifications by dSHERLOCK, ddPCR, and qPCR in terms of CFU.

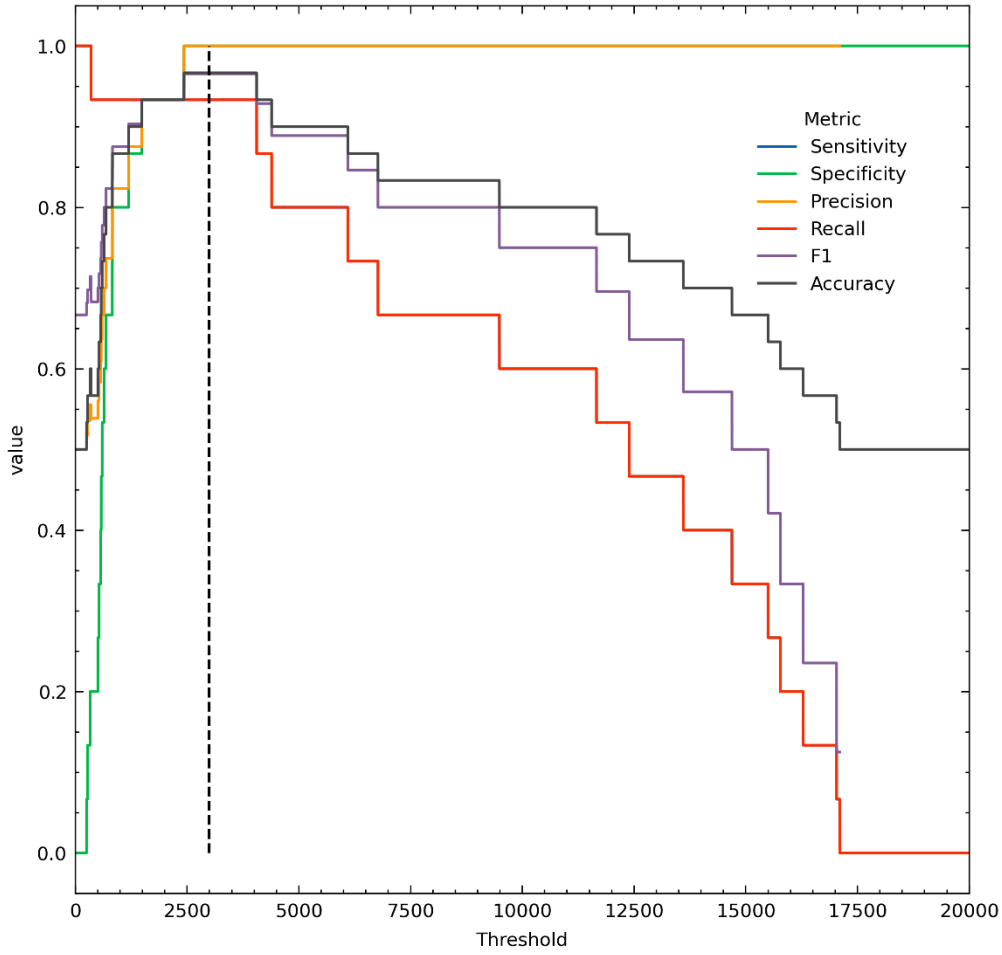
CFU counts were aimed to have three equidistantly logarithmically spaced sample concentrations equal between all the *C. auris* clades.

qPCR, performed before transport to the Wyss Institute, was successfully employed in validating these relationships between the samples, showing three relatively clearly separated groups of measured values,

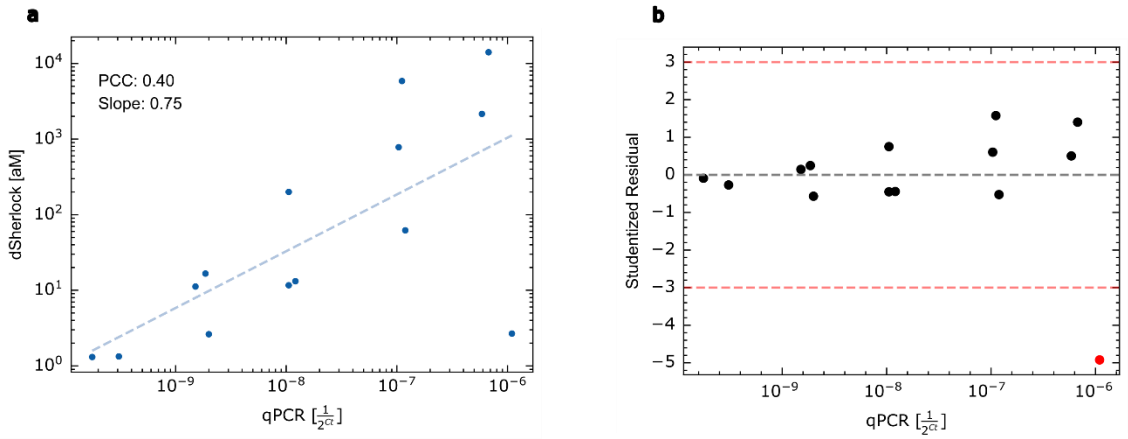
each corresponding to the low, medium or high concentration as determined in terms of CFU (SI Fig 3). dSHERLOCK, like qPCR, identifies clade 1 (purple) samples to have a strikingly low concentration for the high concentration sample and agrees relatively well on the relative ordering of the samples with three major exceptions: the medium concentrations of clades 2 (red) and 3 (green) as well as the high concentration of clade 2 (red).

The comparison of the dSHERLOCK results to digital droplet PCR (ddPCR), performed after transport to the Wyss Institute, reveal a very good agreement on these medium concentrations as well as all other sample concentrations except for the lowest and highest concentration samples. The most likely interpretation of this finding however would be a shift of the linear range of the two methods with respect to each other.

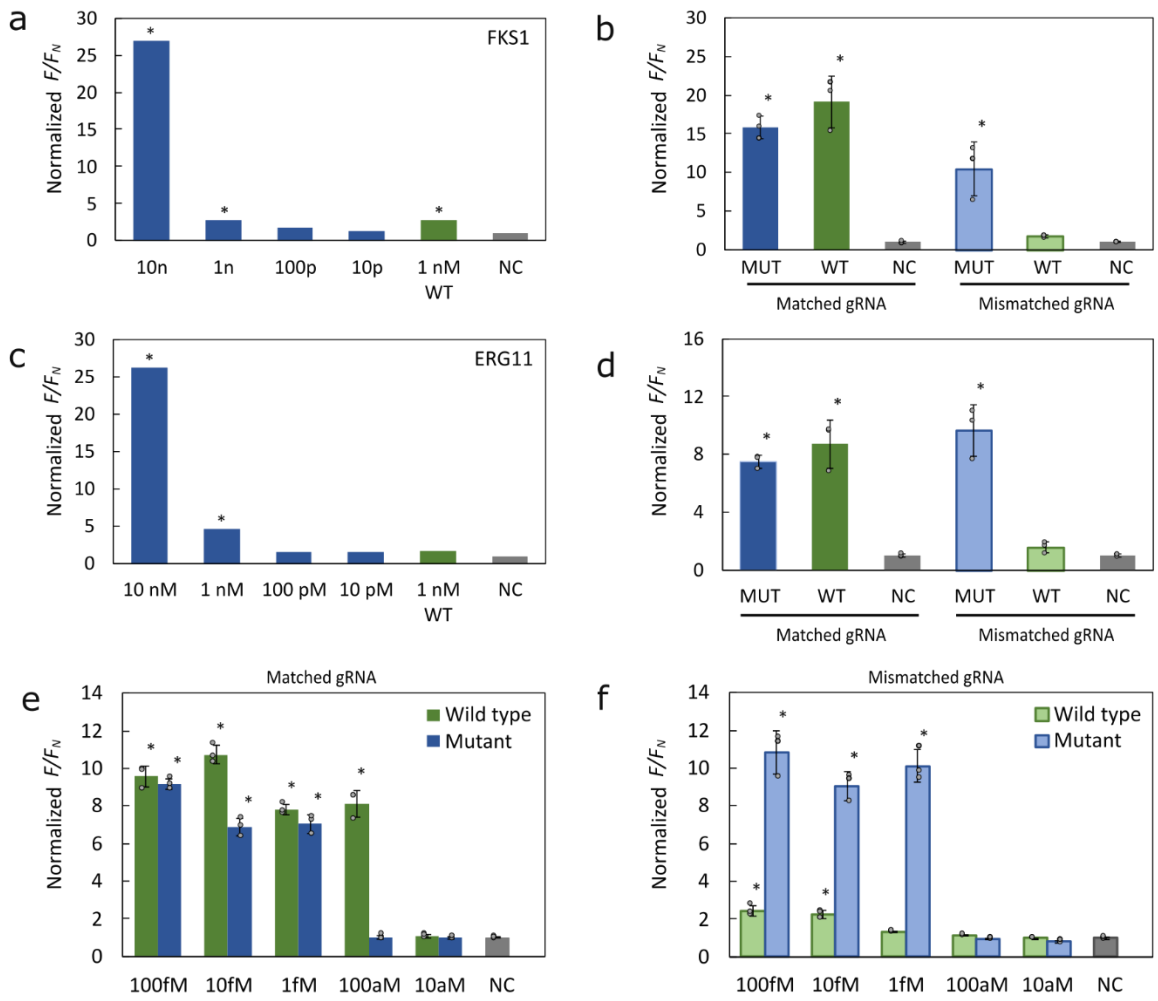
These results combined with the consideration of potentially imperfect transport conditions lead to the conclusion that at least some of the samples must have undergone degradation after CFU determination and qPCR measurement but before dSHERLOCK and ddPCR measurements.



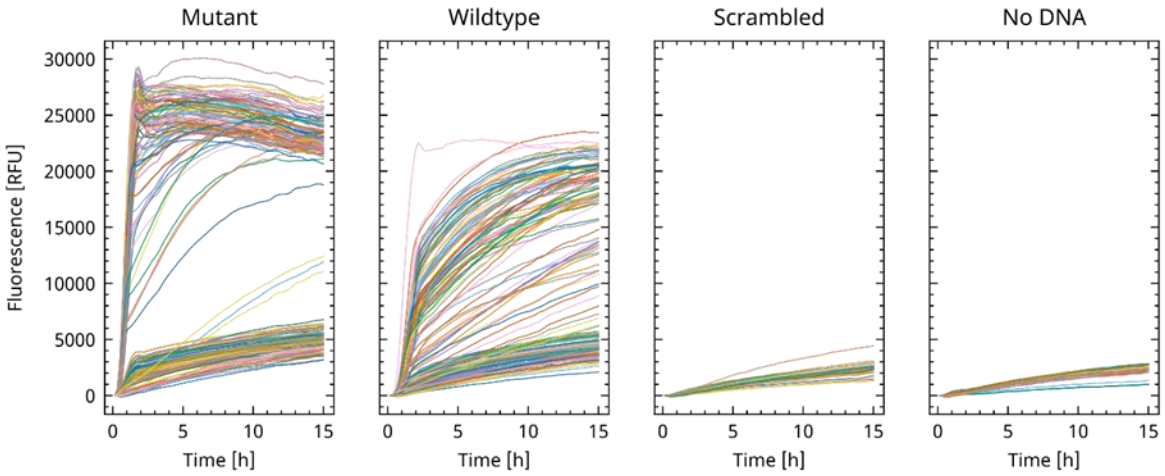
SI Fig 8. Selection of optimal fluorescence threshold dSHERLOCK assays for *C auris* with clinical swabs. Dashed line at the chosen threshold of 3000 RFU corresponds to the optimal performance metrics of the assay. Detection of C. auris is robust to the specific choice of threshold as a number of optimal thresholds are possible, spanning a range of 2500-4000 RFU, without performance deterioration. n=30 samples.



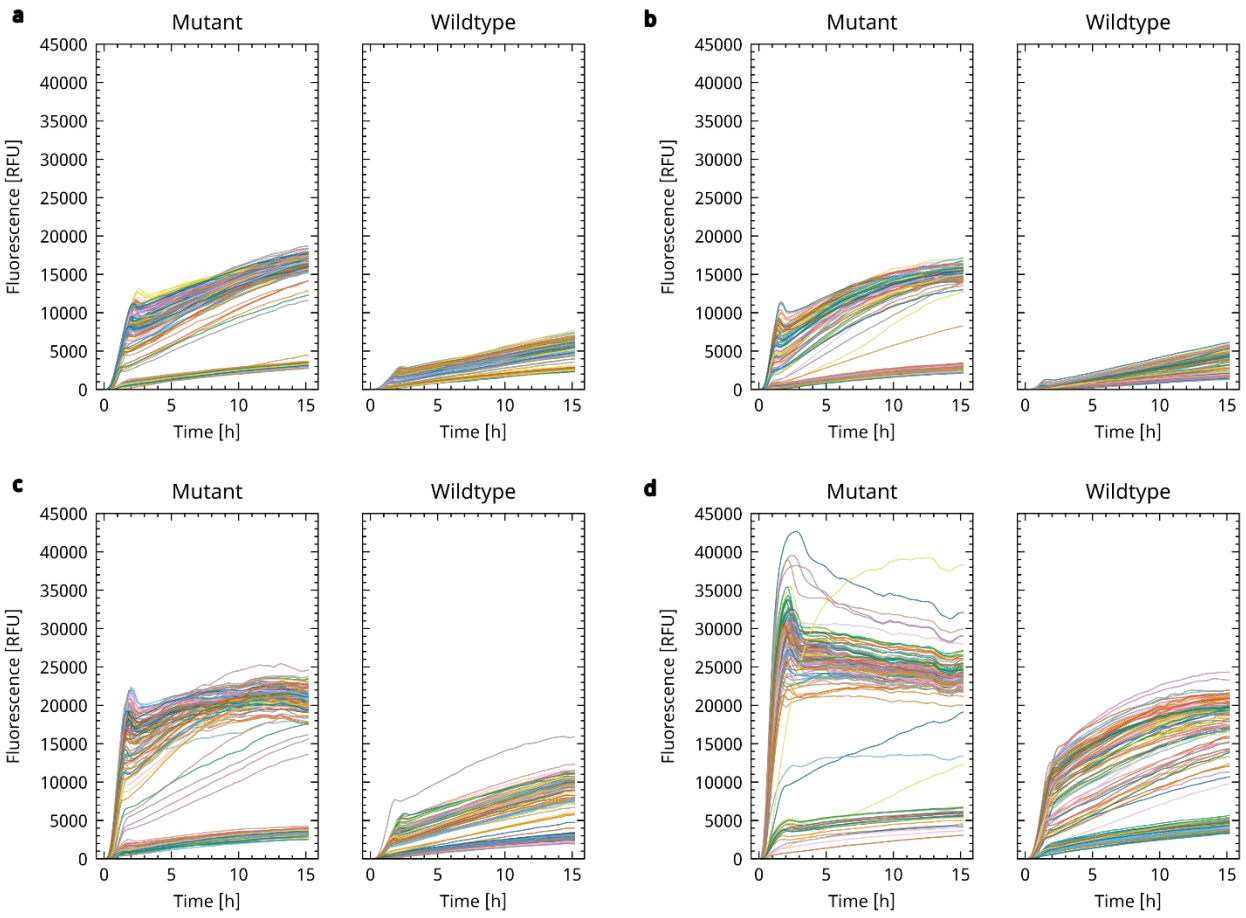
SI Fig 9. Outlier detection on dSHERLOCK quantification of *C. auris* in clinical swabs. a, Correlation between quantification by dSHERLOCK and qPCR including all samples measured as positive by dSHERLOCK and qPCR. Pearson Correlation Coefficient (PCC) was 0.4 indicating a moderate positive correlation. **b,** Studentized residuals for all points in a. Points with studentized residuals with magnitude greater than 3 were determined to be outliers. n=14 positive of 30 samples tested.



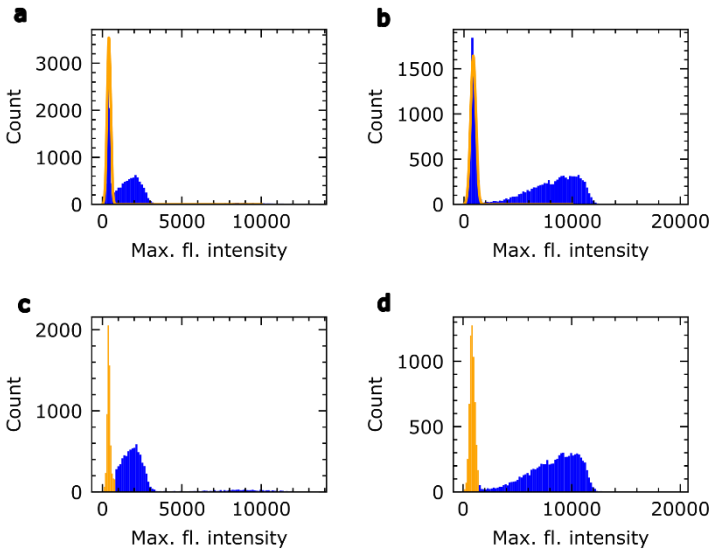
SI Fig 10. Optimization of SHERLOCK FKS1 and ERG11 assay one pot reactions through engineered mutations. **a,** Screen of the sensitivity of FKS1 gRNA matched to the mutant sequence without amplification (90min, n=1), **b,** One-pot screen of the FKS1 assay with matched and mismatched gRNA (1fM, 150min). This shows the additional engineered mismatch in the gRNA knocking out the non-specific signal from the WT DNA, **c,** Screen of the sensitivity of ERG11 gRNA matched to the mutant sequence without amplification (90min, n=1), **d,** One-pot screen of the ERG11 assay with matched and mismatched gRNA (10fM, 150min). This shows the additional engineered mismatch in the gRNA knocking out the signal from the WT DNA, **e,** Sensitivity of gRNA matched to the mutant allele of ERG11, showing detection of both mutant and wild type DNA. **f,** Sensitivity of gRNA having one engineered mismatch to the mutant allele of ERG11, resulting in two mismatches to the wildtype allele and showing specific detection of the mutant. Unless otherwise specified, all data in SI Fig 10 a-f are presented as the mean of technical triplicates (n=3), with error bars representing standard deviation above and below the mean. Fluorescence signal (F) is normalized to the mean of the negative control (F_N); using a threshold of $F/F_N > 2$, positive signals have been marked with an *; MUT- mutant synthetic DNA, WT- wild type synthetic DNA, NC- negative control (water instead of DNA).



SI Fig 11. dSHERLOCK FKS1 assay fluorescence intensity over time. dSHERLOCK's ability to track partitions over time enables deeper insights into the kinetics of reactions by evaluating the change in the fluorescence in individual compartments over time. Scrambled represents a synthetic DNA of a scrambled sequence, equal in length to synthetic DNA targets mutant and wildtype, measured at a sample concentration of 50 fM. No DNA represents samples of pure nuclease-free water without DNA. Intervals between images were 10 min and all reactions were prepared independently in triplicate (n=3 per panel). A random sub-selection of 1% of the approximately 20,000 curves from representative chips is plotted for visibility.



SI Fig 12. Batch effects prohibit the use of thresholds for robust differentiation between alleles. a-b, Batches with low activity cross the threshold of 3000 RFU slower, such that wildtype become undetectable and mutant alleles appear as wildtypes. **c-d,** Batches with high activity contain wildtype reactions that cross the threshold early and with velocities comparing to mutant reactions from low activity batches. Intervals between images were 10 min. A random sub-selection of 1% of the approximately 20,000 curves from each chip is plotted for visibility (representative data from n=8 chips of 54 total chips).



SI Fig 13. Feature extraction and labelling of negative compartments via GRANITE (Gaussian Robust Algorithm for Negative Identification via Thorough Estimation). a-b, a robust gaussian fitting algorithm can be used to reliably identify the distribution of negative compartments via the feature maximum fluorescence intensity in both **(a)** chips loaded with wildtype allele and **(b)** chips loaded with mutant allele. **c-d,** compartments can be labelled as negative by evaluating their probability of being generated by the gaussian-distributed process. Representative data from n=4 chips of 54 total chips.

Bibliography

(1) Piepenburg, O.; Williams, C. H.; Stemple, D. L.; Armes, N. A. DNA Detection Using Recombination Proteins. *PLOS Biology* **2006**, *4* (7), e204. DOI: 10.1371/journal.pbio.0040204

(2) Özay, B.; McCalla, S. E. A review of reaction enhancement strategies for isothermal nucleic acid amplification reactions. *Sensors and Actuators Reports* **2021**, *3*, 100033. DOI: https://doi.org/10.1016/j.snr.2021.100033